

Zirconium(IV) Tris(phosphinoamide) Complexes as a Tripodal-Type Metalloligand: A Route to Zr–M (M = Cu, Mo, Pt) Heterodimetallic Complexes

Takashi Sue,^[a] Yusuke Sunada,^[a,b] and Hideo Nagashima*^[a,b]

Keywords: Phosphinoamide / Heterodimetallic / Tripodal ligands

Treatment of ZrCl₄ with 3 equiv. of Li(PPh₂NR) (R = *t*Bu, *i*Pr) gives tris(phosphinoamide)zirconium complexes, (PPh₂NR)₃ZrCl [R = *t*Bu (**1a**), *i*Pr (**1b**)], in high yield. Crystal structures of **1a,b** show that three phosphorus atoms are coordinated to the zirconium center in the solid state, whereas variable temperature NMR studies indicate a reversible coordination/dissociation process of three phosphorus atoms in the solution state. Reaction of **1a,b** with CuCl give rise to the formation of Zr–Cu heterodimetallic complexes, ClCu(Ph₂PNR)₃ZrCl [R = *t*Bu (**2a**), *i*Pr (**2b**)]. The molecular structures of **2a,b** show that the Cu atom adopts a pseudotetrahedral coordination geometry with tripodal phosphorus moieties and a chlorine atom, whereas the ligand arrangement around the Zr atom is trigonal bipyramidal with the linear Cl–Zr–Cu axis at

the apical site. A Zr–Mo heterodimetallic complex, (CO)₃Mo(Ph₂PN*i*Pr)₃ZrCl (**3**), is synthesized from **1b** and Mo(CO)₃(CH₃CN)₃, in which the ligands around the Mo center are arranged octahedrally, and three phosphorus moieties are coordinated in the *fac*-P₃ fashion. The reaction of **1b** with a square planar Pt^{II} precursor, such as (COD)PtCl₂, is unique and gives (κ²-Ph₂PN*i*Pr)Pt(Ph₂PN*i*Pr)₂ZrCl₃ (**4**), which is the first example of a Zr–Pt zwitterionic heterodimetallic complex. The reaction involves intramolecular migration of two chlorine atoms from Pt to Zr as well as that of a Ph₂PN*i*Pr moiety from Zr to Pt.

(© Wiley-VCH Verlag GmbH & Co. KGaA, 69451 Weinheim, Germany, 2007)

1. Introduction

It is well-known in coordination chemistry that ligand design is important for the synthesis of transition-metal complexes with unique structures and properties. Phosphanes are one of the most investigated ligands, especially in their application to homogeneous catalysis. Numerous monodentate and bidentate phosphane ligands have been developed, and their ligation to appropriate transition metals has contributed to the opening of new aspects in catalytic transformations of organic molecules and polymers.^[1] Electronic and steric effects of these phosphane ligands are well-documented by using Tolman's χ values and cone angles for monodentate phosphanes and bite angles for bidentate phosphane ligands.^[2] Thus, the chemical properties of most transition-metal complexes having monodentate and/or bidentate phosphane ligands are predictable in modern organometallic chemistry. Although relatively little has been studied compared with chemistry of mono- and bidentate phosphane ligands, tridentate phosphane ligands have attracted the attention of organometallic chemists as a re-

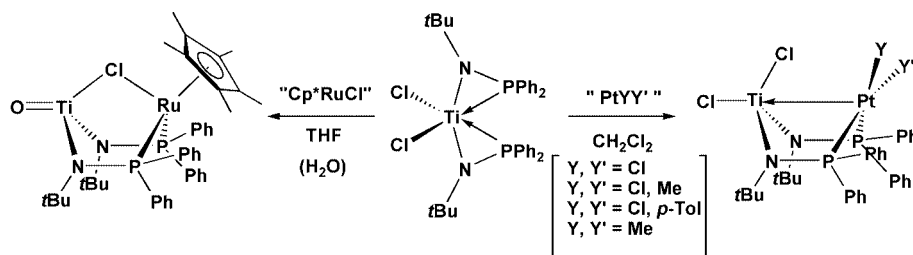
sult of their special structural and chemical properties.^[3] Tridentate tertiary phosphane ligands can be classified into two types according to their preferred coordination geometries: one is the *fac*-P₃ (tripodal) coordination mode, whereas the other is the *mer*-P₃ coordination mode. The phosphane 1,1,1-tris[(diphenylphosphanyl)methyl]ethane (triphos) is the best-known *fac*-P₃ tripodal-type phosphane ligand for transition metals.^[4] For instance, treatment of triphos with CuCl or Mo(CO)₃(CH₃CN)₃ reportedly gives (triphos)CuCl^[4a] or (triphos)Mo(CO)₃, respectively.^[4b] These examples clearly demonstrate that the tripodal ligands rigidly coordinate to a single transition-metal center in the *fac*-P₃ fashion so as to stabilize the mononuclear transition-metal complexes with tetrahedral and octahedral coordination geometries. This feature is different from the *mer*-P₃ ligands that are often used to stabilize a multimetallic framework, which bridges over the dual metals by virtue of its structural flexibility.

An interesting recent development used to control the electronic properties of the phosphane ligand is the introduction of a Lewis acid center in the ligand backbone.^[5] As shown in Figure 1, the “amphoteric ligand” reported by Labinger is a typical example, in which both the Lewis acidic R₂Al moieties and Lewis basic R₂P units are included in one molecule; unique reactivity of the aluminum phosphinoamide Ph₂PN*t*BuAlEt₂ was discovered in the reaction with several transition-metal carbonyls.^[6,7] The bi-

[a] Graduate School of Engineering Sciences, Kyushu University Kasuga, Fukuoka, 816-8580 Japan

[b] Institute for Materials Chemistry and Engineering, Kasuga, Fukuoka, 816-8580 Japan
E-mail: nagashima@cm.kyushu-u.ac.jp

Supporting information for this article is available on the WWW under <http://www.eurjic.org> or from the author.



Scheme 1.

dentate version of the amphoteric ligand was lately reported by Bourissou and coworkers who reported the synthesis of diphosphanlyborane (*o*-*i*Pr₂P-C₆H₃)₂B(Ph) and its ligation to the RhCl moiety in the reaction with [Rh(nbd)Cl]₂.^[8,9] We reported earlier a titanium version of bidentate amphoteric ligands, (Ph₂PNR)₂TiCl₂ (R = *t*Bu, *i*Pr), which are good precursors to Ti–Pt and Ti–Ru heterodimetallic complexes, YY'Pt(Ph₂PN*t*Bu)₂TiCl₂ (Y, Y' = Cl; Y = Me, Y' = Cl; Y = *p*-Tol, Y' = Cl; Y, Y' = Me) and Cp*Ru(μ-Cl)(Ph₂PN*t*Bu)₂Ti = O as shown in Scheme 1.^[10] The Ti–Pt complexes have a trigonal bipyramidal titanium and a square planar platinum center,^[10a] whereas the Ti–Ru complex has titanium and ruthenium atoms with trigonal bipyramidal and tetrahedral geometries, respectively.^[10b] Synthesis of a tridentate amphoteric ligand was examined by the design of the *fac*-P₃ tripodal-type compounds containing a cyclopentadienyl or tris(pyrazolyl)hydroborate zirconium moiety in the molecule; Cp*Zr(OCH₂PPh₂)₃ or TpZr(OCH₂PPh₂)₃ acts as a tripodal-like ligand in Cp*Zr(OCH₂PPh₂)₃Ni(CO), Cp*Zr(OCH₂PPh₂)₃RhMe, and TpZr(OCH₂PPh₂)₃Mo(CO)₃.^[11]

We were interested in the fact that the cyclopentadienyl group in previous examples of the *fac*-P₃ tripodal-type amphoteric ligands reduced the Lewis acidity of the zirconium center. As described above, we synthesized the titanium phosphinoamides as a bidentate amphoteric ligand, which was successfully ligated to organoruthenium or platinum species to give the corresponding Ti–Ru and Ti–Pt complexes. Of interest are the structures of these heterodimetallic complexes: the Ti–Ru compound has a bridging chlorine atom, whereas the existence of a Pt→Ti dative bond is suggested from the crystal structure of the Ti–Pt complexes. The Lewis acidity of the titanium center is probably the reason for these structural features. In this context, we examined the synthesis of (PPh₂NR)₃TiCl (R = *i*Pr, *t*Bu) by the reaction of TiCl₄ with 3 equiv. of LiNRPPH₂; however, (PPh₂NR)₂TiCl₂ was the only product at room temperature and only a small amount of the species assignable to the desired (PPh₂NR)₃TiCl (R = *i*Pr, *t*Bu) was detectable by NMR spectroscopy when the reaction mixture was heated at 70 °C. In sharp contrast, the reaction of 3 equiv. of lithium phosphinoamide with ZrCl₄ successfully led to the formation of tris(phosphinoamide)zirconium, (PPh₂NR)₃ZrCl [R = *t*Bu (**1a**), *i*Pr (**1b**)]. In this paper, we describe the preparation, molecular structure, and solution dynamics of **1a,b** and their coordination behavior to several late transition metals. The heterodimetallic complexes ClCu(Ph₂PNR)₃ZrCl and (CO)₃Mo(Ph₂PN*i*Pr)₃ZrCl showed that these zirconium phosphinoamides behave as a *fac*-P₃ tripodal ligand which effectively stabilizes the late-transition-metal complexes with tetrahedral and octahedral geometries. A unique reaction involving complicated intermetallic ligand rearrangement occurred in the reaction of **1b** with (COD)PtCl₂, which afforded a zwitterionic dimetallic complex, (κ²-Ph₂PN*i*Pr)Pt(Ph₂PN*i*Pr)₂ZrCl₃ (**4**).

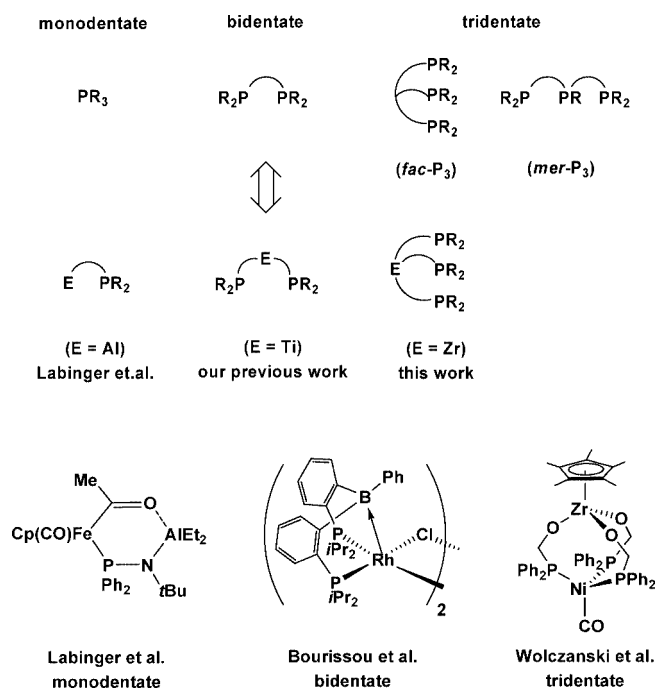


Figure 1. Monodentate, bidentate, and tridentate phosphorus ligands containing a Lewis acidic center.

2. Results and Discussion

2.1 Synthesis and Characterization of Tris(phosphinoamide)-zirconium Complexes (Ph₂PN*t*Bu)₃ZrCl (**1a**) and (Ph₂PN*i*Pr)₃ZrCl (**1b**)

Treatment of 3 equiv. of Li(Ph₂PNR) (R = *t*Bu, *i*Pr) with zirconium tetrachloride in THF afforded tris(phosphinoamide)zirconium complexes, (Ph₂PNR)₃ZrCl [R = *t*Bu (**1a**), *i*Pr (**1b**)], in 86 and 84% yield, respectively, as colorless crys-

tals (Scheme 2). A single ³¹P NMR resonance appeared for **1a,b** at –11.8 and –12.0 ppm, respectively, which were 34.4 and 46.5 ppm shifted to higher field relative to that of the phosphinoamide ligands Ph₂PNH*t*Bu and Ph₂PNH*i*Pr.^[12] Although dynamic behavior was observed, as described later in detail, ¹H and ¹³C NMR spectroscopy clearly showed signals assignable to Ph₂P and *t*Bu or *i*Pr groups. The molecular structures of **1a,b** were determined by X-ray diffraction analysis and are shown in Figure 2; representative bond lengths and angles for **1a,b** are summarized in Table 1. The asymmetric unit of **1a** contains three crystallographically independent but chemically equivalent molecules. Ambiguous value of the Flack parameter (0.42) suggests the structure of **1a** is inversion twinned, which is sometimes seen in a trigonal space group. There is a three-fold axis along with the Zr–Cl bond in the solid-state structure of all three independent molecules of **1a**. One of the molecular structures of **1a** is described in Figure 2. Three phosphinoamide ligands are connected to the zirconium center by a Zr–N bond and all of the three phosphorus moieties are coordinated. Both **1a,b** assume a distorted tetrahedral geometry with one chlorine atom and three centers of the N–P bonds. In the solid-state structure, all three phosphorus atoms are oriented away from the chlorine atom, and no isomer was found in the crystal. The N–P bond lengths are comparable to those seen in Eisen's zirconium tetrakis(phosphinoamide) complex, Zr(Ph₂PNPh)₄,^[13] our previously reported titanium complexes, (Ph₂PNR)₂TiCl₂ (R = *t*Bu, *i*Pr), and other known phosphinoamide or related complexes.^[14] The Zr–N bond lengths around 2.15 Å are slightly longer than those found in previously reported zirconium amide complexes,^[15] whereas the Zr–P bond lengths are somewhat shorter than those of known zirconium phosphane complexes.^[16]

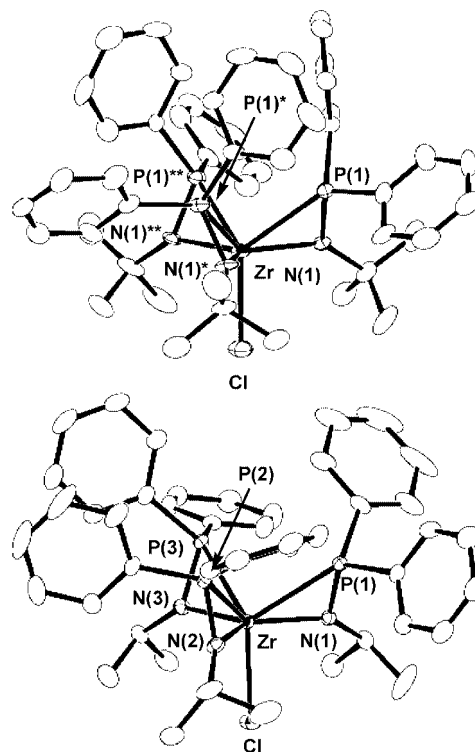
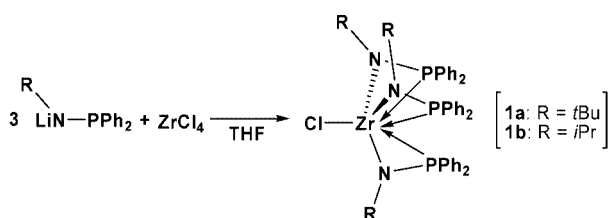


Figure 2. Molecular structures of (Ph₂PN*t*Bu)₃ZrCl (**1a**) (top) (Ph₂PN*i*Pr)₃ZrCl (**1b**) (bottom) with 50% probability ellipsoids. Hydrogen atoms are omitted for clarity.

Although all of the three phosphorus atoms are bonded with the zirconium center in the solid state, NMR spectroscopic studies suggested a dynamic coordination/dissociation process of these three phosphorus atoms that is similar to that of titanium phosphinoamide, (Ph₂PNR)₂TiCl₂,^[10a] and Zr(Ph₂PNPh)₄.^[13] In a representative example, ¹H NMR spectra of **1a** are dependent on the temperature measured: at room temperature, three broad signals at δ = 6.99–7.17 ppm and one singlet at δ = 1.47 ppm were seen, which are assignable to the protons of the Ph group and the methyl portion of the *t*Bu group. At –90 °C, the spectrum consists of six signals at δ = 6.53 (m, 2 H), 6.66 (t, 2 H), 6.95 (t, 1 H), 7.20 (t, 2 H), 7.24 (m, 2 H), and 7.29 (t, 1 H) ppm and a slightly broadened singlet at δ = 1.37 ppm, which are assignable to two sets of phenyl signals



Scheme 2.

Table 1. Representative bond lengths and angles for **1a,b**.

Bond lengths [Å]			Bond angles [°]		
	1a	1b		1a	1b
Zr–Cl(1)	2.505(2) [2.488(2), 2.525(2)]	2.4865(9)	Cl–Zr–N(1)	91.09(13) [91.07(12), 89.70(11)]	86.28(7)
Zr–N(1)	2.183(6) [2.181(4), 2.180(3)]	2.150(2)	Cl–Zr–N(2)		86.18(8)
Zr–N(2)		2.137(2)	Cl–Zr–N(3)		93.81(8)
Zr–N(3)		2.101(2)	N(1)–Zr–N(2)	120.0(2) [119.9(2), 120.2(2)]	133.29(10)
Zr–P(1)	2.626(2) [2.617(2), 2.608(2)]	2.6659(9)	N(1)–Zr–N(3)		117.07(10)
Zr–P(2)		2.6577(9)	N(2)–Zr–N(3)		109.40(10)
Zr–P(3)		2.6516(9)	N(1)–Zr–P(1)	38.87(14) [39.22(13), 39.21(12)]	38.09(7)
N(1)–P(1)	1.654(5) [1.662(5), 1.656(4)]	1.645(2)	N(2)–Zr–P(2)		38.30(8)
N(2)–P(2)		1.648(3)	N(3)–Zr–P(3)		38.64(7)
N(3)–P(3)		1.656(2)			

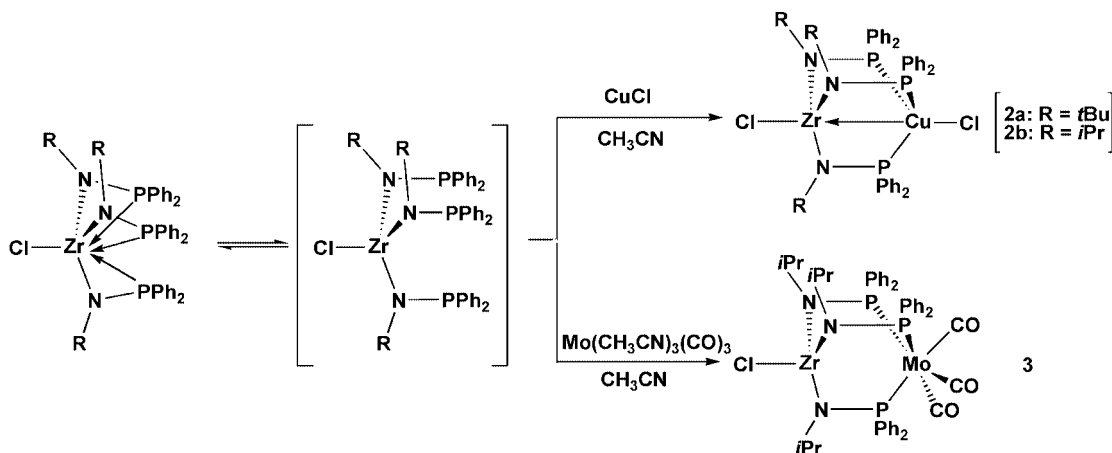
of the *ortho*-, *meta*-, *para*-, *meta*-, *ortho*-, and *para* protons, respectively, and a signal for the *t*Bu group. ^1H NMR spectroscopic resonances due to the phenyl moieties were unequivocally assigned by a ^1H - ^1H selective decoupling measurement. The spectrum is explained by the existence of three magnetically equivalent phosphinoamide ligands, in which two phenyl groups bonded with each phosphorus atom are inequivalent. Similar variable temperature NMR studies of **1b** also showed dynamic behavior; two signals due to the Ph group [$\delta = 7.12$ – 7.17 (m, 12 H), 7.22 – 7.26 (m, 18 H) ppm] appeared at room temperature, which were broadened at -90°C to show three broad signals. Similarly, the methyl and methine signals of the *i*Pr group were gradually broadened at lower temperatures, and only a single set of broad signals was seen even at -90°C . Because **1b** is not very soluble in CD_2Cl_2 at low temperatures, the well-resolved spectra below -90°C , in which two doublets due to the inequivalent methyl groups should appear, were unable to be obtained because of technical problems. These spectral changes are consistent with the fact that phosphorus atoms are coordinated to the zirconium center at lower temperatures, whereas reversible dissociation takes place at higher temperatures in solution states; this is favorable for the possible usage of **1** as a tripodal metalloligand as described later.^[17]

In close analogy to these results, Eisen and coworkers reported the preparation and structure determination of $\text{Zr}(\text{Ph}_2\text{PNPh})_4$, which also showed dynamic behavior in variable temperature NMR studies.^[13] The four phosphinoamide ligands are bonded to the zirconium atom by Zr–N and Zr←P bonds in the solid state. In solution, the coordination of the phosphorus atoms is reversible. Although the synthetic method of Eisen's complex is similar to that of **1**, neither $\text{Zr}(\text{Ph}_2\text{PN}i\text{Bu})_4$ nor $\text{Zr}(\text{Ph}_2\text{PN}i\text{Pr})_4$ was detected in our experiments. As a representative experiment, ZrCl_4 was treated with 4 equiv. of $\text{Li}(\text{Ph}_2\text{PN}i\text{Pr})$ in THF at room temperature overnight; ^1H and ^{31}P NMR spectra of the crude product showed the formation of **1b** as a single product; $\text{Zr}(\text{Ph}_2\text{PN}i\text{Pr})_4$ was not detected. This is presumably attributable to the steric bulkiness of the *t*Bu and *i*Pr groups, which prevents the reaction of **1** to the correspond-

ing zirconium tetrakis(phosphinoamide). It should be noted that we have never seen the formation of $(\text{Ph}_2\text{PNR})_2\text{ZrCl}_2$ ($\text{R} = i\text{Bu}, i\text{Pr}$) even in the reaction of ZrCl_4 with less than 2 equiv. of $\text{Li}(\text{Ph}_2\text{PNR})$, though Zhang et al. recently reported the synthesis of bis(phosphinoamide)zirconium complexes, $(\text{Ph}_2\text{PNR})_2\text{ZrCl}_2$ ($\text{R} = t\text{Bu}, \text{Ph}$), by the reaction of 2 equiv. of $\text{Li}(\text{Ph}_2\text{PNR})$ ($\text{R} = t\text{Bu}, \text{Ph}$) with ZrCl_4 ; no detailed spectroscopic data were described.^[18] Repeated attempts to reproduce the result of Zhang were unsuccessful. In a typical example, 2 equiv. of $\text{Li}(\text{Ph}_2\text{PN}i\text{Bu})$ was reacted with ZrCl_4 in THF from which only complex **1a** was obtained in 30–50% yield and unreacted ZrCl_4 was recovered as a THF adduct. This is interesting in comparison with our previous result that the reaction of TiCl_4 with 2 equiv. of $\text{Li}(\text{Ph}_2\text{PNR})$ resulted in the exclusive formation of $(\text{Ph}_2\text{PNR})_2\text{TiCl}_2$.

2.2 Use of **1** as a Tripodal-Type Metalloligand: Construction of Zr–Cu and Zr–Mo Heterodimetallic Complexes $\text{ClCu}(\text{Ph}_2\text{PNR})_3\text{ZrCl}$ [$\text{R} = t\text{Bu}$ (**2a**), *i*Pr (**2b**)] and $(\text{CO})_3\text{Mo}(\text{Ph}_2\text{PN}i\text{Pr})_3\text{ZrCl}$ (**3**)

As described above, the fluxional behavior of **1** in the variable temperature ^1H NMR spectroscopic studies suggested that **1** was a *fac*- P_3 tripodal-type metalloligand. It is known that the *fac*- P_3 tripodal-type is suitable as the ligand of complexes with tetrahedral or octahedral geometry.^[3] As a representative model of a tetrahedral complex, Cu^{I} complexes were prepared. Treatment of **1** with 1 equiv. of CuCl in CH_3CN at room temperature afforded Zr–Cu heterodimetallic complexes, $\text{ClCu}(\text{Ph}_2\text{PNR})_3\text{ZrCl}$ [$\text{R} = t\text{Bu}$ (**2a**), *i*Pr (**2b**)], as yellow crystals in 78 and 82% yield, respectively (Scheme 3). The products were unequivocally characterized by NMR spectroscopy, in which no dynamic behavior was visible in the temperature range from -90 to 30°C . In a typical example, the ^1H NMR spectrum of **2a** gave signals due to the *ortho*-, *meta*-, and *para* protons of six magnetically equivalent Ph groups in an integral ratio of 12:12:6, and one singlet at $\delta = 1.50$ ppm, which is assignable to the methyl protons of the *t*Bu group. In the ^{13}C NMR spec-



Scheme 3.

trum, four signals at $\delta = 127.9$ (*meta*-Ph), 129.5 (*para*-Ph), 132.8 (*ortho*-Ph), and 134.5 (*ipso*-Ph) ppm are observed, which are assignable to the six magnetically equivalent phenyl groups, along with two signals at $\delta = 34.8$ (CMe₃) and 61.8 (CMe₃) ppm due to the three magnetically equivalent *t*Bu groups. This clearly demonstrates the C_{3v} symmetry of the molecule. A singlet appeared at $\delta = -30.6$ ppm in the ³¹P NMR spectrum of **2a**; peak broadening due to the interaction with the quadrupolar copper center is good evidence of the coordination of three phosphorus moieties to the Cu atom. Spectral data of **2b** is analogous to those of **2a** in the points that three Ph₂PN*t*Pr ligands are magnetically equivalent (the integral ratio of methyl and methine protons of *i*Pr and three Ph protons is 18:3:12:12:6) and broadening of the ³¹P NMR spectroscopic resonance ($\delta = -11.2$ ppm) is ascribed to the coordination of the phosphorus moiety to the copper center. The C_{3v} symmetric structure deduced from these spectroscopic features is confirmed by X-ray diffraction analysis of **2a,b** of which the ORTEP drawings are shown in Figure 3, and selected bond lengths and angles are summarized in Table 2.

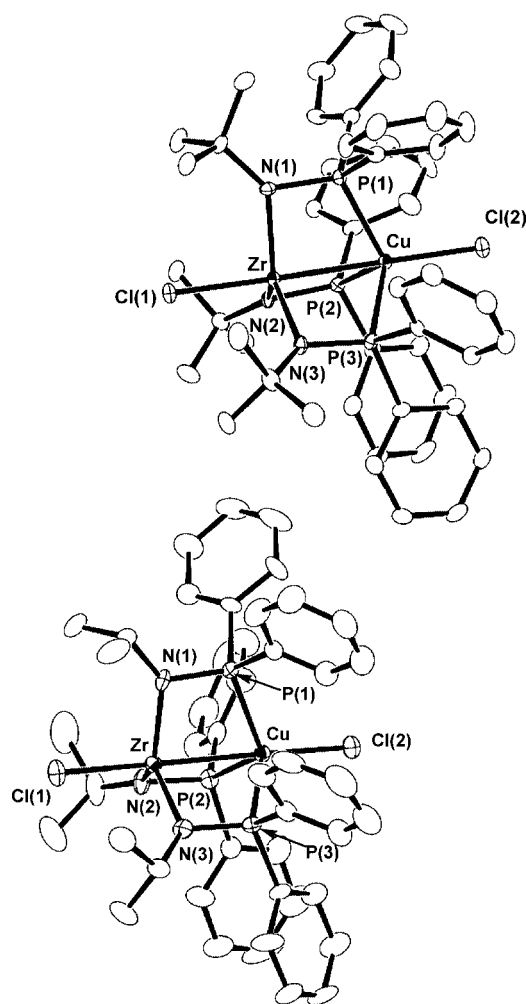


Figure 3. Molecular structures of ClCu(Ph₂PN*t*Bu)₃ZrCl (**2a**) (top) and ClCu(Ph₂PN*i*Pr)₃ZrCl (**2b**) (bottom) with 50% probability ellipsoids. Hydrogen atoms are omitted for clarity.

The asymmetric unit of **2b** contains two crystallographically independent but chemically equivalent molecules. Bond lengths and angles of the second molecule are given in brackets in Table 2. The molecular structures show that two metal centers are linked by three phosphinoamide ligands. The zirconium center adopts a trigonal bipyramidal coordination geometry with the three nitrogen atoms in the basal position and the Cl(1)–Zr–Cu as the apical axis. The sum of the equatorial angles around the zirconium atom is ca. 357°. Alternatively, the geometry around the copper is distorted tetrahedrally because of the effective stabilization of tetrahedral geometry given by tripodal-type P₃ coordination. The Cl(1)–Zr–Cu–Cl(2) axis is arranged linearly, the bent angles of Cl(1) and Cl(2) from the Zr–Cu axis are 0.77(2)° and 3.12(4)°, respectively, in **2a**. The N–P bond lengths of **2a,b** are approximately 0.1 Å shorter than the normal N–P single bonds, but comparable to those of starting zirconium complexes **1a,b**, which reflect the partial N–P double bond character. This was supported by the sum of the three angles at the N atom (359.3–359.9°), which is close to the theoretical value of 360° for the planar sp²-hybridized nitrogen atom. The shorter bond lengths of N–P were also observed in our Ti–Pt and Ti–Ru phosphinoamide complexes,^[10] Zr(Ph₂PNPh)₄,^[13] and related complexes.^[14] The Cu–P [2.3126(12)–2.3626(11) Å] bond lengths are slightly longer than those of (triphos)CuCl (2.282–2.299 Å),^[4c] but comparable to related copper phosphane complexes such as (PPh₃)₃CuCl (2.348 Å).^[19]

Reaction of **1b** with an octahedrally arranged molybdenum precursor led to the formation of Zr–Mo heterodimetallic complex **3** (Scheme 3). In **3**, ligands around the molybdenum center are arranged octahedrally, to which the zirconium phosphinoamide moieties are coordinated in a facial coordination mode. Treatment of **1b** with Mo(CO)₃(CH₃CN)₃ in CH₂Cl₂ at room temperature resulted in the replacement of the CH₃CN ligands by three phosphorus atoms of **1b** to give a Zr–Mo heterodimetallic complex, (CO)₃Mo(Ph₂PN*i*Pr)₃ZrCl (**3**), in 70% yield as pale yellow crystals. The ¹H NMR spectrum of **3** showed signals for three magnetically equivalent Ph₂PN*i*Pr moieties, which indicates the C_{3v} symmetric structure of **3** in solution. No dynamic behavior was observed in variable temperature NMR spectroscopic experiments. The ³¹P NMR spectrum of **3** showed a singlet at $\delta = 36.3$ ppm, which is low-field shifted by ca. 20 ppm relative to (triphos)Mo(CO)₃ ($\delta = 16.8$ ppm). The IR spectrum of **3** shows characteristic C≡O stretching bands at 1987 and 1913 cm⁻¹, which is 50–70 cm⁻¹ shifted to higher frequencies relative to those of (triphos)Mo(CO)₃ (1937, 1844 cm⁻¹).^[4b] The back-donation from molybdenum to the π* orbital of CO in **3** is apparently weaker than that in (triphos)Mo(CO)₃. There are two possible explanations for this: one is direct through-space interaction between Lewis acidic Zr and Mo atoms; the other is through-bond interaction by way of the Zr–N–P–Mo bond.^[20]

The molecular structure determined by X-ray diffraction analysis is depicted in Figure 4, and representative bond lengths and angles are summarized in Table 2. The two

Table 2. Representative bond lengths and angles for dimetallic complexes.

	Bond lengths [Å]				Bond angles [°]				
	2a	2b ^[a]	3	4	2a	2b ^[a]	3	4	
Zr–M	2.6069(7)	2.6854(6)	2.9741(5)	2.964(4)	Cl(1)–Zr–M	179.23(2)	178.93(3)	180	163.01(4)
Zr–Cl(1)	2.4314(11)	2.4026(10)	2.4427(12)	2.390(2)	Zr–M–Cl(2)	176.88(4)	174.99(3)		
Zr–Cl(2)		2.4048(13)		2.506(2)	N(1)–Zr–N(2)	118.44(14)	116.79(13)	119.66(9)	99.8(2)
Zr–Cl(3)				2.4936(14)	N(1)–Zr–N(3)	120.34(14)	118.90(14)	119.72(10)	
Zr–N(1)	2.149(2)	2.100(3)	2.114(2)	2.140(3)	N(2)–Zr–N(3)	120.29(12)	121.04(14)	119.68(8)	
Zr–N(2)	2.156(4)	2.108(4)	2.115(2)	2.181(4)	P(1)–M–P(2)	85.94(3)	83.48(3)	100.16(2)	101.03(4)
Zr–N(3)	2.157(3)	2.107(3)	2.113(2)		P(1)–M–P(3)	84.92(2)	81.59(2)	100.20(2)	106.94(4)
M–P(1)	2.3626(11)	2.3146(10)	2.5787(5)	2.2439(11)	P(2)–M–P(3)	83.22(3)	80.85(3)	100.17(2)	145.57(12)
M–P(2)	2.3356(12)	2.3306(12)	2.5796(8)	2.3270(11)	Zr–N(1)–P(1)	93.1(2)	98.5(2)	99.08(8)	102.2(2)
M–P(3)	2.3408(12)	2.3458(11)	2.5783(7)	2.2548(11)	Zr–N(2)–P(2)	95.0(2)	99.8(2)	99.08(8)	105.0(2)
N(1)–P(1)	1.665(3)	1.666(3)	1.671(2)	1.641(4)	Zr–N(3)–P(3)	95.3(2)	99.6(2)	99.08(8)	
N(2)–P(2)	1.649(3)	1.671(3)	1.671(2)	1.641(4)			[99.0(2)]		
N(3)–P(3)	1.659(3)	1.668(3)	1.671(2)	1.615(4)			[99.0(2)]		

[a] The asymmetric unit of **2b** consists of two crystallographically independent but chemically equivalent molecules. Bond lengths and angles of the second molecule are given in brackets.

metal centers are connected by three phosphinoamide bridges and three phosphorus atoms are coordinated to the molybdenum center in a *fac*-P₃ fashion. The Mo–P bond lengths of **3** [2.5783(7)–2.5796(8) Å] are slightly longer relative to those found in previously reported (triphos)-Mo(CO)₃ [2.516(1) Å],^[4b] whereas C–O bond lengths of 1.140(3) Å are comparable to those of (triphos)-

Mo(CO)₃ [1.155(3) Å].^[4b] The Mo–Zr and Mo–P distances suggest that the above-described shift of the $\nu(\text{C}\equiv\text{O})$ band to higher frequencies can be better explained by through-bond interactions.

2.3 Construction of Zr–Pt Heterodimetallic Complexes with the Use of Pt^{II} Precursors that Do Not Provide Suitable Coordination Geometries for *fac*-P₃ Ligands

In the above-described two types of heterodimetallic complexes, the zirconium phosphinoamides act as the *fac*-P₃ tripodal-type ligand. The tetrahedral geometry of the Cu^I and octahedral structure of the Mo⁰ are suitable for the *fac*-P₃ tripodal-type coordination. One question concerns the fate of the zirconium phosphinoamides in the reaction with the second metal complex fragment that does not have the appropriate coordination geometry for the *fac*-P₃ tripodal-type coordination. To resolve this question, we chose a square-planar arranged Pt^{II} precursor as the reactant in the reaction with **1**. Treatment of **1b** with (COD)PtCl₂ in CH₂Cl₂ at room temperature for 1 h afforded a novel Zr–Pt heterodimetallic complex, (κ^2 -Ph₂PNiPr)₂Pt(Ph₂PNiPr)₂-ZrCl₃(**4**) in 75% yield (Scheme 4). The ³¹P NMR spectrum of **4** showed the presence of three different phosphorus atoms with a satellite signal due to the coupling with ¹⁹⁵Pt, $\delta = 12.9$ ($J_{\text{P,P}} = 6.7$, 286 Hz, $J_{\text{Pt,P}} = 3153$ Hz), 3.4 ($J_{\text{P,P}} = 6.7$, 13.9 Hz, $J_{\text{Pt,P}} = 3403$ Hz), and -32.5 ppm ($J_{\text{P,P}} = 13.9$, 286 Hz, $J_{\text{Pt,P}} = 1578$ Hz). In contrast to the C_{3v} symmetric structures of the Zr–Cu and Zr–Mo complexes giving a sin-

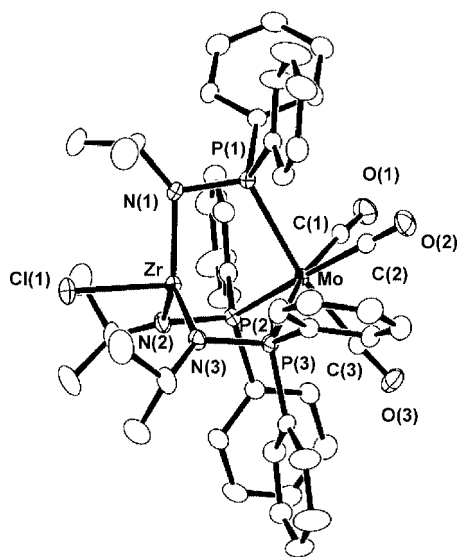
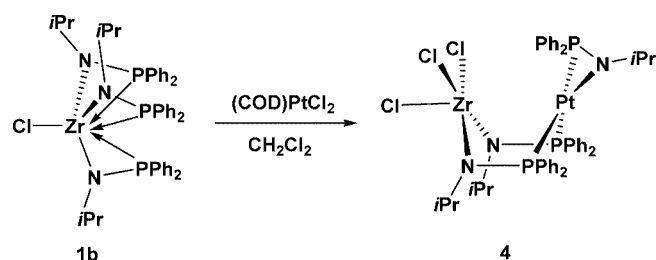


Figure 4. Molecular structure of (CO)₃Mo(Ph₂PNiPr)₃ZrCl (**3**) with 50% probability ellipsoids. Hydrogen atoms are omitted for clarity.

gle ³¹P NMR spectroscopic resonance, the ³¹P NMR spectrum of **4** clearly demonstrates that three Ph₂PN*i*Pr ligands in **4** are magnetically inequivalent and the complex has no symmetry. The nonsymmetric structure of **4** is also supported by the ¹H NMR spectrum of **4**; in a typical example, there exists three doublets at δ = 0.71, 1.15, and 1.45 ppm, which are due to the methyl protons of the *i*Pr group. It is noteworthy that one of them (δ = 0.71 ppm) is significantly shifted to a higher field (*vide infra*).



Scheme 4.

The molecular structure of **4** was established by X-ray study. Figure 5 shows the ORTEP view of **4** and selected bond lengths and angles of **4** are listed in Table 2. Two metal centers are linked by two phosphinoamide bridges in a boat form similar to Ti–Pt and Ti–Ru phosphinoamide complexes. Ligand arrangement around the zirconium atom is pseudooctahedral with two nitrogen atoms and two chlorine atoms at the basal plane and Cl(1) and Pt at the apical position. Geometry around the platinum atom is distorted square planar with the Pt atom out of the plane defined by P(1), P(2), and the center of N(3)–P(3) (ca. 0.077 Å). A similar distorted structure was also observed in YY'Pt(Ph₂PN*t*Bu)₂TiCl₂ complexes in which the Pt atom is out of the plane by ca. 0.181–0.328 Å. The N(3)–P(3) bond length of 1.615(4) Å is ca. 0.03 Å shorter than those of the bridging phosphinoamide ligands, which indicates that there is a slightly increased double bond character of the N(3)–P(3) bond. The ligand arrangement indicates that **4** is formally considered to have a zwitterionic form with Zr^{IV-} and Pt^{II+} centers. To the best of our knowledge, this is the first example of a zwitterionic Zr–Pt heterodimetallic complex. The molecular structure provided clues for understanding the NMR spectroscopic data, which included three magnetically inequivalent methyl and methine signals of the *i*Pr group that were observed in the ¹H NMR spectrum and three ³¹P NMR spectroscopic resonances with different chemical shifts and ³¹P–¹⁹⁵Pt coupling constants. The nonsymmetric structure of **4** is reasonable in giving three doublets at δ = 0.71, 1.15, and 1.45 ppm that are due to the methyl protons of the *i*Pr group. An unusual upfield shift of one of the three doublets due to the methyl group in the *i*Pr moieties can be ascribed to the methyl proton of the *i*Pr of κ²-coordinated phosphinoamide moiety, which is effectively shielded by one of the phenyl rings of the PPh₂ group of the bridging phosphinoamide ligand. The signal at δ = 3.4 ppm in the ³¹P NMR spectrum is *trans* to the N

atom of the κ²-coordinated phosphinoamide and the other two are *trans* to each other. The value of each coupling constant is consistent with this interpretation.

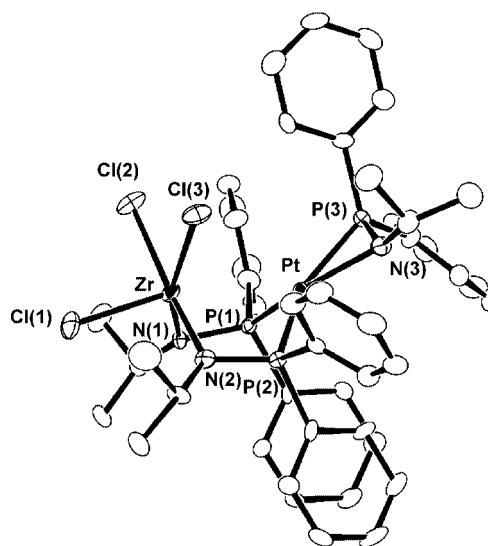
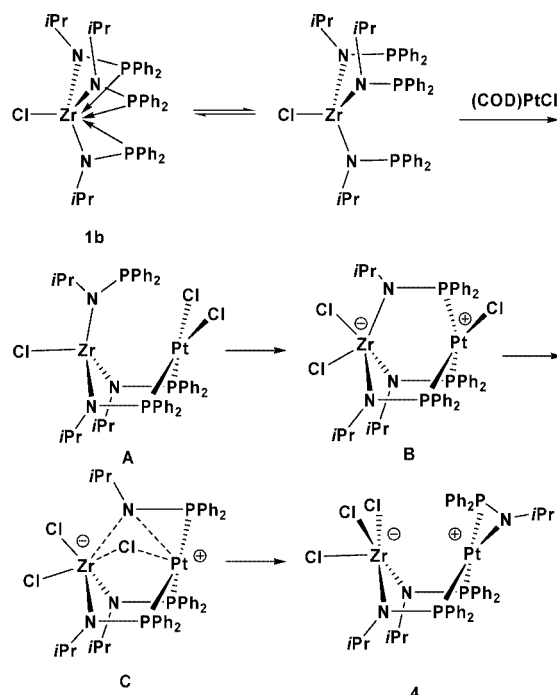


Figure 5. Molecular structure of (κ²-Ph₂PN*i*Pr)Pt(Ph₂PN*i*Pr)₂-ZrCl₃(**4**) with 50% probability ellipsoids. Hydrogen atoms are omitted for clarity.

This unusual ligand rearrangement in the reaction of **1b** with a square planar platinum complex fragment provided some mechanistic insight. The reaction is likely to occur intramolecularly and the ligand migration is internuclear. The dimetallic structure of **4**, in which the Zr and Pt exist close enough to exchange their individual ligands, is the key to accomplish the rearrangement. The possible mechanism is illustrated in Scheme 5. Three phosphorus atoms of zircono-



Scheme 5.

nium phosphinoamide **1b** reversibly dissociate to their uncoordinated forms in solution and two of them react with a square-planar Pt^{II} species to form **A**. Coordination of the remaining phosphorus atom to the Pt^{II} center results in internuclear migration of a chlorine atom from Pt to Zr to give zwitterionic intermediate **B**. The tricyclic structure of **B** generates significant ring strain that triggers the cleavage and recombination of the Zr–N and Pt–Cl bonds to form **4**. These results clearly demonstrate that zirconium phosphinoamides **1a,b** behave as *fac*-P₃ tripodal-type metalloligands in the reaction with transition metals that are able to attain a tetrahedral or octahedral geometry while coordinated to the metal center with a square planar structure. This geometry is unfavorable for the coordination of the tripodal-type ligand and as such an internuclear ligand arrangement is induced to release the ring strain of the primarily formed intermediates.

3. Concluding Remarks

As described above, we attained success in the preparation of tris(phosphinoamide)zirconium complexes, (Ph₂PNR)₃ZrCl [R = *t*Bu (**1a**), *i*Pr (**1b**)], which reacted with a second metal complex fragment to form heterodimetallic complexes, ClCu(Ph₂PNR)₃ZrCl (**2**) and (CO)₃Mo(Ph₂PN*i*Pr)₃ZrCl (**3**). In the Zr–Cu and Zr–Mo complexes, the coordination geometry around the late-transition-metal center is defined as pseudotetrahedral and octahedral, respectively, owing to the effective coordination of they P₃-moiety of **1** in the tripodal fashion. The reaction of **1b** with square planar arranged (COD)PtCl₂ is unique and gives a zwitterionic heterodimetallic complex (κ^2 -Ph₂PN*i*Pr)Pt(Ph₂PN*i*Pr)₂ZrCl₂ (**4**); this reaction involves intramolecular migration of two chlorine atoms from Pt to Zr as well as that of a *i*PrNPPH₂ moiety from Zr to Pt. In heterodimetallic complexes **2–4**, the Lewis acidic zirconium and the late-transition-metal atoms are closely located; this realized the internuclear ligand arrangement seen in the formation of **4**. The driving force for the rearrangement can be attributed to the fact that the hard chlorine atom preferred the hard zirconium center, whereas the soft phosphinoamide ligand preferred the soft platinum atom. Of interest is the possible dative interaction of the late transition metal to the zirconium atom. As reported earlier, we proposed the Ti←Pt interaction in the YY'Pt(Ph₂PN*t*Bu)₂TiCl₂ complexes from the crystal structures. There is an occupied d_{z²} orbital in the platinum atom, and this possibly interacted with the Lewis acidic titanium center. The Ti←Pt bond lengths decrease in the order Cl₂Pt(Ph₂PN*t*Bu)₂TiCl₂ [2.8358(6) Å] > MeClPt(Ph₂PN*t*Bu)₂TiCl₂ [2.7547(10) Å] > Me₂Pt(Ph₂PN*t*Bu)₂TiCl₂ [2.6860(11) Å]; this is explained by assuming that the higher electron dense platinum complex moiety can make a stronger dative bond interaction. The molecular structure of **2** revealed that the Zr–Cu bond length of **2a** [2.6069(7) Å] is slightly shorter than the sum of the van der Waals radii of Zr and Cu (ca. 2.74 Å)^[21] (ca. 95% of the sum of the radii). In contrast, the Zr–Mo and

Zr–Pt distances of 2.9741(5) and 2.964(4) Å in complexes **3** and **4**, respectively, are nearly identical to the sum of the van der Waals radii of Zr–Mo and Zr–Pt (ca. 3.05 Å)^[21] (98 and 97% of the sum of the radii, respectively). The Rh–B interaction is proposed in Bourissou's complex, {(*o*-*i*Pr₂P-C₆H₃)₂B(Ph)]RhCl}₂, from chemical shifts of the ¹¹B NMR spectroscopic resonance and the Rh–B distance found from X-ray crystallography. This was supported by DFT calculations {BP86/[CEP-31G(Rh), 6-31G*(other elements)]}, in which bonding interaction was observed at the HOMO of the complex.^[8] However, our preliminary theoretical calculations (single-point calculation of the structure of **2a**/HF/LanL2DZ) did not provide clear evidence for the bonding interaction at the HOMO level. Thus, further theoretical studies with a higher functional level, including those of **3**, **4**, previously reported Ti–Pt heterodimetallic complexes, and related complexes, should be performed to discuss metal–metal interactions.

In summary, **1** is useful as a metalloligand for the formation of Zr–M heterodimetallic compounds, though the coordination mode of **1** was dependent on the preferred coordination environment of the second transition–metal centers. Current efforts are directed towards the synthesis of novel heterodimetallic complexes with several second transition-metal complex fragments having other coordination geometries. Their systematic results, including structural properties and dynamic behaviors, are expected to open the way to construct novel heterodimetallic complexes with unique structures, electronic properties, and reactivities.

Experimental Section

General: Manipulation of air- and moisture-sensitive organometallic compounds was carried out under a dry argon atmosphere by using standard Schlenk tube techniques associated with a high-vacuum line, or with the nitrogen filled glove box. All solvents were distilled from appropriate drying reagents prior to use (THF, hexane; Ph₂CO/Na, CH₃CN, CH₂Cl₂; CaH₂). ¹H, ¹³C, and ³¹P NMR spectra were recorded with a JEOL Lambda 600 or a Lambda 400 spectrometer at ambient temperature unless otherwise noted. ¹H, ¹³C, and ³¹P NMR chemical shifts (δ values) were given in ppm relative to the solvent signal (¹H, ¹³C) or standard resonances (³¹P; external 85% H₃PO₄). IR spectra were recorded with a JASCO FT/IR-550 spectrometer. Melting points were measured with a Yanaco SMP3 micro melting point apparatus. Elemental analyses were performed by the Elemental Analysis Center, Faculty of Science, Kyushu University, or with a Perkin–Elmer 2400/CHN analyzer. Starting materials, phosphinoamide,^[12] [Mo(CO)₃(CH₃CN)₃],^[22] and (COD)PtCl₂^[23] were synthesized by the method reported in the literature.

(Ph₂PNR)₃ZrCl [R = *t*Bu (1a**), *i*Pr (**1b**):** In a 100-mL Schlenk tube, Ph₂PNH*t*Bu (2589 mg, 10.06 mmol) was dissolved in THF (30 mL). A hexane solution of *n*BuLi (1.56 M, 6.5 mL, 10.14 mmol) was added to the solution at –78 °C, and the solution was slowly warmed to room temperature. After stirring at room temperature for 3 h, the mixture was cooled to –78 °C and a THF (15 mL) solution of ZrCl₄ (800 mg, 3.43 mmol) was added dropwise. The slightly yellow solution turned off white in color and a white solid precipitated. After 12 h, all of the volatiles were removed under

vacuum, and the formed crude product was dissolved in CH₂Cl₂ (20 mL). The insoluble materials were filtered off through a G3 filter, and the resulting filtrate was concentrated to a volume of 5 mL. Hexane (20 mL) was added to this supersaturated CH₂Cl₂ solution. The desired product was obtained as colorless crystals in 86% yield (2580 mg, 2.88 mmol). In a similar fashion, **1b** was obtained in 84% yield as colorless crystals. **1a**: M.p. 108 °C (dec). ¹H NMR (600 MHz, CD₂Cl₂): δ = 1.47 (s, 27 H, *t*Bu), 6.99–7.17 (br., 30 H, Ph) ppm. ¹³C NMR (150 MHz, CD₂Cl₂): δ = 34.1 (*CMe*₃), 60.0 (m, *CMe*₃), 127.5 (m, *meta*-Ph), 128.8 (*para*-Ph), 133.4 (m, *ortho*-Ph), 136.75 (*ipso*-Ph) ppm. ³¹P{¹H} NMR (243 MHz, CD₂Cl₂): δ = -11.8 (s) ppm. C₄₈H₅₇ClN₃P₃Zr (895.59): calcd. C 64.37, H 6.42, N 4.69; found C 64.14, H 6.42, N 4.45. **1b**: M.p. 107–108 °C (dec). ¹H NMR (600 MHz, CD₂Cl₂): δ = 1.20 [d, *J*_{H,H} = 6.6 Hz, 18 H, (CH₃)₂CH], 3.89 [sept, *J*_{H,H} = 6.6 Hz, 3 H, (CH₃)₂CH], 7.12–7.17 (m, 12 H, *meta*-Ph), 7.22–7.26 (m, 18 H, *ortho* and *para*-Ph) ppm. ¹³C NMR (150 MHz, CD₂Cl₂): δ = 26.8 [(CH₃)₂CH], 53.2 [(CH₃)₂CH], 128.1 (*meta*-Ph), 129.3 (*para*-Ph), 133.4 (m, *ortho*-Ph), 136.9 (m, *ipso*-Ph) ppm. ³¹P{¹H} NMR (243 MHz, CD₂Cl₂): δ = -12.0 (s) ppm. C₄₅H₅₁ClN₃P₃Zr (853.51): calcd. C 63.32, H 6.02, N 4.92; found C 63.34, H 6.52, N 5.40.^[24]

ClCu(Ph₂PNR)₃ZrCl [R = *t*Bu (2a), *i*Pr (2b)]: A 20-mL Schlenk tube was charged with **1a** (44 mg, 0.050 mmol) and CuCl (5 mg, 0.051 mmol), and the atmosphere was replaced by argon. The mixture was dissolved in CH₃CN (5 mL). The color of the solution changed immediately from colorless to yellow, from which a yellow precipitate was separated. After removal of the solvent in vacuo, the solid was washed with hexane (3 × 2 mL). The crude product was dissolved in warm CH₂Cl₂, and the insoluble materials (unreacted CuCl) were filtered off. The filtrate was cooled to -30 °C to form yellow microcrystals of **2a** in 78% yield (38 mg, 0.038 mmol). In a similar fashion, **1b** was obtained in 82% yield as yellow microcrystals. **2a**: M.p. 116–117 °C (dec). ¹H NMR (600 MHz, CD₂Cl₂): δ = 1.50 (s, 27 H, *t*Bu), 6.96 (t, *J* = 7.4 Hz, 12 H, *meta*-Ph), 7.15 (t, *J* = 7.4 Hz, 6 H, *para*-Ph), 7.42 (br., 12 H, *ortho*-Ph) ppm. ¹³C NMR (150 MHz, CD₂Cl₂): δ = 34.8 (*CMe*₃), 61.8 (m, *CMe*₃), 127.9 (*meta*-Ph), 129.5 (*para*-Ph), 132.8 (*ortho*-Ph), 134.5 (m, *ipso*-Ph) ppm. ³¹P{¹H} NMR (243 MHz, CD₂Cl₂): δ = -30.6 (br) ppm. C₄₈H₅₇Cl₂CuN₃P₃Zr (994.59): calcd. C 57.97, H 5.78, N 4.22; found C 57.51, H 5.94, N 4.32. **2b**: M.p. 117–118 °C (dec). ¹H NMR (600 MHz, CD₂Cl₂): δ = 1.38 [d, *J*_{H,H} = 6.6 Hz, 18 H, (CH₃)₂CH], 3.85 [m, 3 H, (CH₃)₂CH], 6.98 (t, *J*_{H,H} = 7.7 Hz, 12 H, *meta*-Ph), 7.19 (t, *J*_{H,H} = 7.7 Hz, 6 H, *para*-Ph), 7.34 (br., 12 H, *ortho*-Ph) ppm. ¹³C NMR (150 MHz, CD₂Cl₂): δ = 27.2 [(CH₃)₂CH], 53.2 [(CH₃)₂CH], 128.1 (*meta*-Ph), 130.0 (*para*-Ph), 133.7 (m, *ortho*-Ph), 134.8 (m, *ipso*-Ph) ppm. ³¹P{¹H} NMR (243 MHz, CD₂Cl₂): δ = -11.2 (br) ppm. C₄₅H₅₁Cl₂CuN₃P₃Zr (952.52): calcd. C 56.74, H 5.40, N 4.41; found C 56.87, H 5.80, N 4.59.

(CO)₃Mo(Ph₂PNiPr)₃ZrCl (3): A 20-mL Schlenk tube was charged with **1b** (428 mg, 0.501 mmol) and Mo(CO)₃(CH₃CN)₃ (155 mg, 0.511 mmol), and the atmosphere was replaced by argon. The mixture was dissolved in CH₂Cl₂ (5 mL), and the solution was stirred at room temperature for 1 h. The color of the reaction mixture changed from yellow to red. The solution was kept at -30 °C to form pale yellow microcrystals of **3** in 70% yield (365 mg, 0.353 mmol). M.p. 227–228 °C (dec). ¹H NMR (600 MHz, CD₂Cl₂): δ = 1.11 [d, *J*_{H,H} = 6.8 Hz, 18 H, (CH₃)₂CH], 3.67 [m, 3 H, (CH₃)₂CH], 7.25–7.28 (m, 12 H, *meta*-Ph), 7.36–7.41 (m, 18 H, *para* and *ortho*-Ph) ppm. ¹³C NMR (150 MHz, CD₂Cl₂): δ = 26.0 [(CH₃)₂CH], 53.0 [(CH₃)₂CH], 128.9 (m, *meta*-Ph), 129.8 (*para*-Ph), 133.4 (m, *ortho*-Ph), 138.0 (m, *ipso*-Ph), 218.3 (m, CO) ppm. ³¹P{¹H} NMR (243 MHz, CD₂Cl₂): δ = 36.3 (s) ppm. IR (KBr

pellet): ν̄ = 1987 (C≡O), 1913 (C≡O) cm⁻¹. C₄₈H₅₁Cl₂MoN₃O₃P₃Zr (1033.49): calcd. C 55.78, H 4.97, N 4.07; found C 55.48, H 4.91, N 4.00.

(κ²-Ph₂PNiPr)Pt(Ph₂PNiPr)₂ZrCl₃ (4): A 20-mL Schlenk tube was charged with **1b** (50 mg, 0.059 mmol) and (COD)PtCl₂ (21 mg, 0.056 mmol), and the atmosphere was replaced by argon. The mixture was dissolved in CH₂Cl₂ (5 mL), and the solution was stirred at room temperature for 1 h. The color of the reaction mixture changed from yellow to red. The solution was cooled to -30 °C to form pale yellow crystals of **4** in 75% yield (47 mg, 0.042 mmol). M.p. 126–128 °C (dec). ¹H NMR (600 MHz, CD₂Cl₂): δ = 0.71 [d, *J*_{H,H} = 6.8 Hz, 6 H, (CH₃)₂CH], 1.15 [d, *J*_{H,H} = 6.0 Hz, 6 H, (CH₃)₂CH], 1.45 [d, *J*_{H,H} = 6.0 Hz, 6 H, (CH₃)₂CH], 2.97 [m, 1 H, (CH₃)₂CH], 3.47 [m, 1 H, (CH₃)₂CH], 3.62 [m, 1 H, (CH₃)₂CH], 6.75–6.80 (m, 4 H, Ph), 6.90–6.97 (m, 4 H, Ph), 7.07–7.12 (m, 2 H, Ph), 7.13–7.17 (m, 4 H, Ph), 7.22–7.27 (m, 2 H, Ph), 7.37–7.42 (m, 4 H, Ph), 7.51–7.60 (m, 10 H, Ph) ppm. ¹³C NMR (150 MHz, CD₂Cl₂): δ = 25.2 [(CH₃)₂CH], 25.8 [(CH₃)₂CH], 27.0 [(CH₃)₂CH], 49.2 [(CH₃)₂CH], 54.2 [(CH₃)₂CH], 54.7 [(CH₃)₂CH], 127.5 (Ph), 128.2 (Ph), 129.0 (Ph), 130.5 (Ph), 130.7 (Ph), 133.0 (Ph), 133.1 (Ph), 133.4 (Ph), 134.1 (Ph) ppm. ³¹P{¹H} NMR (243 MHz, CD₂Cl₂): δ = 12.9 (dd, *J*_{P,P} = 6.7, 286 Hz, *J*_{Pt,P} = 3153 Hz), 3.4 (dd, *J*_{P,P} = 6.7, 13.9 Hz, *J*_{Pt,P} = 3403 Hz), -32.5 (dd, *J*_{P,P} = 13.9, 286 Hz, *J*_{Pt,P} = 1578 Hz) ppm. C₄₅H₅₁Cl₃N₃P₃Zr (1119.51): calcd. C 48.28, H 4.59, N 3.75; found C 48.14, H 4.66, N 3.68.

Table 3. Crystallographic data for zirconium phosphinoamides.

	1a	1b
Empirical formula	C ₄₈ H ₅₇ ClN ₃ P ₃ Zr	C ₄₅ H ₅₁ ClN ₃ P ₃ Zr
Formula weight	895.59	853.51
Crystal system	trigonal	monoclinic
Lattice type	primitive	primitive
Space group	P3 (#143)	P2 ₁ /n (#14)
<i>a</i> [Å]	19.4576(14)	11.293(2)
<i>b</i> [Å]	19.4576(14)	16.724(3)
<i>c</i> [Å]	10.8143(10)	22.575(4)
<i>α</i> [°]	90	90
<i>β</i> [°]	90	93.930(2)
<i>γ</i> [°]	120	90
Volume [Å ³]	3545.7(5)	4253.6(12)
<i>Z</i> value	3	4
<i>D</i> _{calcd.} [g cm ⁻³]	1.258	1.333
<i>F</i> (000)	1404.00	1776.00
μ(Mo-K _α) [cm ⁻¹]	4.249	4.686
Crystal color, habit	colorless, prism	colorless, platelet
Crystal dimensions [mm]	0.15 × 0.05 × 0.02	0.25 × 0.15 × 0.08
No. observations (all reflections)	10782	9605
No. variables	506	529
Reflection/parameter ratio	21.31	18.16
<i>R</i> (all reflections)	0.0825	0.0705
<i>R</i> ₁ [<i>I</i> > 2.00σ(<i>I</i>)] ^[a]	0.0757	0.0466
<i>wR</i> ₂ (all reflections) ^[b]	0.1890	0.1494
GOF	1.114	1.006
Flack parameter	0.42(5)	
Max shift/error in final cycle	0.000	0.000
Maximum peak in final diff. map [e Å ⁻³]	4.30	1.23
Minimum peak in final diff. map [e Å ⁻³]	-0.75	-0.76

[a] *R*₁ = Σ|*F*_o| - |*F*_c|/Σ|*F*_o|. [b] *wR*₂ = [Σ{*w*(*F*_o² - *F*_c²)/Σ{*w*(*F*_o²)^{1/2}}]^{1/2}.

Table 4. Crystallographic tables for the heterodimetallic complexes.

	2a	2b	3	4
Empirical formula	C ₄₈ H ₅₇ Cl ₂ N ₃ P ₃ CuZr	C ₄₅ H ₅₁ ClN ₃ P ₃ CuZr·CH ₂ Cl ₂	C ₄₈ H ₅₇ ClO ₃ N ₃ P ₃ MoZr·1/4C ₆ H ₆	C ₄₅ H ₅₁ Cl ₃ N ₃ P ₃ PtZr
Formula weight	994.59	987.96	1033.49	1119.51
Crystal system	triclinic	triclinic	trigonal	monoclinic
Lattice type	primitive	primitive	R-centered	primitive
Space group	<i>P</i> $\bar{1}$ (#2)	<i>P</i> $\bar{1}$ (#2)	<i>R</i> $\bar{3}$ (#148)	<i>P</i> 2 ₁ / <i>n</i> (#14)
<i>a</i> [Å]	10.968(2)	10.9996(12)	14.516(3)	11.539(2)
<i>b</i> [Å]	11.948(2)	21.564(2)	14.516(3)	23.527(4)
<i>c</i> [Å]	19.980(4)	21.801(2)	39.098(7)	16.727(3)
α [°]	79.863(9)	66.326(3)	90	90
β [°]	84.577(9)	83.226(4)	90	92.090(2)
γ [°]	63.397(7)	85.984(4)	120	90
Volume [Å ³]	2304.2(7)	4701.4(8)	7135(2)	4538.1(13)
<i>Z</i> value	2	4	6	4
<i>D</i> _{calcd.} [g cm ⁻³]	1.433	1.396	1.477	1.638
<i>F</i> (000)	1028.00	2028.00	3240.00	2224.00
μ (Mo- <i>K</i> α) [cm ⁻¹]	9.443	9.799	6.839	36.137
Crystal color, habit	yellow, chip	yellow, block	yellow, block	yellow, chip
Crystal dimensions [mm]	0.20 × 0.08 × 0.05	0.20 × 0.18 × 0.10	0.20 × 0.15 × 0.05	0.20 × 0.09 × 0.08
No. observations (all reflections)	10146	20685	3630	10368
No. variables	580	1024	194	506
Reflection/parameter ratio	17.49	20.20	18.71	20.49
<i>R</i> (all reflections) ^[a]	0.0765	0.0733	0.0403	0.0515
<i>R</i> ₁ [<i>I</i> > 2.00σ(<i>I</i>)] ^[b]	0.0535	0.0572	0.0379	0.0454
<i>wR</i> ₂ (all reflections)	0.1675	0.1359	0.0942	0.0855
GOF	1.005	1.067	1.125	1.223
Max shift/error in final cycle	0.000	0.001	0.000	0.002
Maximum peak in final diff. map [e Å ⁻³]	1.62	1.13	0.80	3.73
Minimum peak in final diff. map [e Å ⁻³]	-0.92	-1.58	-1.07	-1.43

[a] $R_1 = \sum |F_o| - |F_c| / \sum |F_o|$. [b] $wR_2 = [\sum \{w(F_o^2 - F_c^2)^2\} / \sum \{w(F_o^2)\}]^{1/2}$.

X-ray Data Collection and Reduction: Single crystals of all complexes were grown from CH₂Cl₂/pentane. X-ray crystallography was performed with a Rigaku Saturn CCD area detector with graphite monochromated Mo-*K* α radiation ($\lambda = 0.71070$ Å). The reflection data were collected at 123(2) K by using ω scan in the θ range of $3.1 \leq \theta \leq 27.5^\circ$ (**1a**), $3.0 \leq \theta \leq 27.5^\circ$ (**1b**), $3.0 \leq \theta \leq 27.5^\circ$ (**2a**), $3.1 \leq \theta \leq 27.5^\circ$ (**2b**), $3.1 \leq \theta \leq 27.5^\circ$ (**3**), $3.1 \leq \theta \leq 27.5^\circ$ (**4**). The data obtained were processed with Crystal-Clear (Rigaku) on a Pentium computer, and were corrected for Lorentz and polarization effects. The structures were solved by direct methods (SIR 97^[25] for **1a,b**, and **2b**, SIR 92^[26] for **2a**, **3**, and **4**) and expanded by using Fourier techniques.^[27] The non-hydrogen atoms were refined anisotropically, and the hydrogen atoms by using the riding model. The final cycle of full-matrix least-squares refinement on *F*² was based on 10782 observed reflections and 563 variable parameters for **1a**, 9605 observed reflections and 529 variable parameters for **1b**, 10146 observed reflections and 580 variable parameters for **2a**, 20685 observed reflections and 1113 variable parameters for **2b**, 10383 observed reflections and 599 variable parameters for **3**, and on 10368 observed reflections and 556 variable parameters for **4**. Neutral atom scattering factors were taken from Cromer and Waber.^[28] All calculations were performed with the Crystal-Structure^[29,30] crystallographic software package. Details of the final refinement are summarized in Tables 3 and 4, and the numbering scheme employed is shown in Figures 2, 3, 4, and 5 which was drawn with ORTEP at 50% probability ellipsoids. Unsatisfactory quality of the crystal in the crystallographic analysis of **1a** provided two large residual densities near the Zr atom. However, the data

obtained are reliable enough to discuss the atom connectivity, bond lengths, and angles. CCDC-632038 (**1a**), -632039 (**1b**), -632040 (**2a**), -632041 (**2b**), -632042 (**3**), and -632043 (**4**) contain the supplementary crystallographic data for this paper. These data can be obtained free of charge from The Cambridge Crystallographic Data Centre via www.ccdc.cam.ac.uk/data_request/cif.

Supporting Information (see footnote on the first page of this article): Variable temperature NMR spectroscopic data (**1a,b**) and ¹H, ¹³C, and ³¹P NMR spectroscopic data (**1a,b**, **2a,b**, **3**, **4**).

Acknowledgments

This work was supported by the Ministry of Education, Culture, Sports, Science and Technology, Japan by Grant-in-Aid for Scientific Research on Priority Areas (No. 15036253 and 16033246), "Reaction Control of Dynamic Complexes".

- [1] a) P. Dierkes, P. W. N. M. van Leeuwen, *J. Chem. Soc., Dalton Trans.* **1999**, 1519–1529; b) P. W. N. M. van Leeuwen, P. C. J. Kamer, J. N. H. Reek, P. Dierkes, *Chem. Rev.* **2000**, *100*, 2741–2770; c) Z. Freixa, P. W. N. M. van Leeuwen, *Dalton Trans.* **2003**, 1890–1901; d) T. Appleby, J. D. Woollins, *Coord. Chem. Rev.* **2002**, *235*, 121–140; e) D. M. A. Minahan, W. E. Hill, C. A. McAuliffe, *Coord. Chem. Rev.* **1984**, *55*, 31–54; f) R.

- Noyori, *Angew. Chem. Int. Ed.* **2002**, *41*, 2008–2022; g) R. Noyori, T. Ohkuma, *Angew. Chem. Int. Ed.* **2001**, *40*, 40–73.
- [2] C. A. Tolman, *Chem. Rev.* **1977**, *77*, 313–348.
- [3] H. A. Mayer, W. C. Kaska, *Chem. Rev.* **1994**, *94*, 1239–1272.
- [4] a) S. Gambarotta, S. Strologo, C. Floriani, A. Chiesi-Villa, C. Guastini, *Organometallics* **1984**, *3*, 1444–1445; b) O. Walter, T. Klein, G. Huttner, L. Zsolnai, *J. Organomet. Chem.* **1993**, *458*, 63–81; c) A. Muth, O. Walter, G. Huttner, A. Asam, L. Zsolnai, Ch. Emmerrich, *J. Organomet. Chem.* **1994**, *468*, 149–163; d) L. Sacconi, S. Midollini, *J. Chem. Soc., Dalton Trans.* **1972**, 1213–1216; e) D. J. Fife, H. J. Mueh, C. F. Campana, *Acta Crystallogr., Sect. C: Cryst. Struct. Commun.* **1993**, *49*, 1714–1716; f) A. F. Kowalski, M. T. Ashby, *J. Am. Chem. Soc.* **1995**, *117*, 12639–12640.
- [5] It is well-known that the reaction of a Lewis acidic boron center with an appropriate anion gives the corresponding borate. Peters et al. described the synthesis of a new type of bidentate and *fac*-P₃ tripodal phosphanes containing a borate anion, bis or tris[(diphenylphosphanyl)methyl]borate such as [Ph_nB(CH₂PPh₂)_{4-n}]⁻ (*n* = 1, 2). They successfully ligate to various transition metals such as Fe, Co, Ni, Pd and Pt complex fragments. Seccia S. J. Thomas, J. C. Peters, *J. Am. Chem. Soc.* **2001**, *123*, 5100–5101; b) T. A. Betley, J. C. Peters, *Angew. Chem. Int. Ed.* **2003**, *42*, 2385–2389; c) J. C. Thomas, J. C. Peters, *Inorg. Chem.* **2003**, *42*, 5055–5073; d) T. A. Betley, J. C. Peters, *Inorg. Chem.* **2003**, *42*, 5074–5084; e) J. C. Thomas, J. C. Peters, *J. Am. Chem. Soc.* **2003**, *125*, 8870–8888; f) C. C. Lu, J. C. Peters, *J. Am. Chem. Soc.* **2004**, *126*, 15818–15832; g) C. C. Lu, J. C. Peters, *J. Am. Chem. Soc.* **2002**, *124*, 5272–5273; h) see ref.^[9b]; i) J. C. Peters, J. C. Thomas, J. A. Dupont, C. G. Riordan, *Inorg. Synth.* **2004**, *34*, p. 8; j) S. D. Brown, M. P. Mehn, J. C. Peters, *J. Am. Chem. Soc.* **2005**, *127*, 13146–13147; k) C. C. Lu, C. T. Saouma, M. W. Day, J. C. Peters, *J. Am. Chem. Soc.*, DOI: 10.1021/ja0604358; l) S. D. Brown, J. C. Peters, *J. Am. Chem. Soc.* **2005**, *127*, 1913–1923; m) C. C. Lu, J. C. V. Peters, *Inorg. Chem.* **2006**, *45*, 8597–8607; n) J. Li, P. I. Djurovich, B. D. Alleyne, M. Yousufuddin, N. N. Ho, J. C. Peters, R. Bau, M. E. Thompson, *Inorg. Chem.* **2005**, *44*, 1713–1727; o) D. M. Jenkins, J. C. Peters, *J. Am. Chem. Soc.* **2005**, *127*, 7148–7165; p) J. C. Peters, J. D. Feldman, T. D. Tilley, *J. Am. Chem. Soc.* **1999**, *121*, 9871–9872; q) C. M. Thomas, N. P. Mankad, J. C. Peters, *J. Am. Chem. Soc.* **2006**, *128*, 4956–4957; r) C. M. Thomas, J. C. Peters, *Organometallics* **2005**, *24*, 5858–5867; s) J. Li, P. I. Djurovich, B. D. Alleyne, M. Yousufuddin, N. N. Ho, J. C. Thomas, J. C. Peters, R. Bau, M. E. Thompson, *Inorg. Chem.* **2005**, *44*, 1713–1727; t) M. T. Whited, E. Rivard, J. C. Peters, *Chem. Commun.* **2006**, 1613–1615; u) I. R. Shapiro, D. M. Jenkins, J. C. Thomas, M. W. Day, J. C. Peters, *Chem. Commun.* **2001**, 2152–2153; v) A. A. Barney, A. F. Heyduk, D. G. Nocera, *Chem. Commun.* **1999**, 2379–2380.
- [6] a) J. A. Labinger, J. N. Bonfiglio, D. L. Grimmer, S. T. Masuo, E. Shearin, J. S. Miller, *Organometallics* **1983**, *2*, 733–740; b) H. H. Karsch, A. Appelt, F. H. Kohler, G. Muller, *Organometallics* **1985**, *4*, 231–238; c) O. T. Beachley Jr. C. Tessier-Youngs, *Organometallics* **1983**, *2*, 796–801; d) F. Thomas, S. Schluz, M. Nieger, K. Nattinen, *Chem. Eur. J.* **2002**, *8*, 1915–1924; e) D. F. Clemens, D. H. H. Sisler, W. S. Brey, *Inorg. Chem.* **1966**, *5*, 527–533.
- [7] For other Lewis acid containing monodentate ligands, see: S. Bontemps, G. Bouhadir, K. Miqueu, D. Bourissou, *J. Am. Chem. Soc.* **2006**, *128*, 12056–12057.
- [8] S. Bontemps, G. Gornitzka, G. Bouhadir, K. Miqueu, D. Bourissou, *Angew. Chem. Int. Ed.* **2006**, *45*, 1611–1614.
- [9] For other Lewis acid containing bidentate ligands, see: a) L. Turculet, J. D. Feldman, T. D. Tilley, *Organometallics* **2004**, *23*, 2488–2502; b) C. Thomas, J. C. Peters, *Polyhedron* **2004**, *23*, 2901–2913.
- [10] a) H. Nagashima, T. Sue, T. Oda, A. Kanemitsu, T. Matsumoto, Y. Motoyama, Y. Sunada, *Organometallics* **2006**, *25*, 1987–1994; b) Y. Sunada, T. Sue, T. Matsumoto, H. Nagashima, *J. Organomet. Chem.* **2006**, *691*, 3176–3182.
- [11] a) G. S. Ferguson, P. T. Wolczanski, L. Párkányi, M. C. Zonneville, *Organometallics* **1988**, *7*, 1967–1979; b) G. S. Ferguson, P. T. Wolczanski, *Organometallics* **1985**, *4*, 1601–1605; c) O. Köhl, S. Joachim, J. Sieler, E. Hey-Hawkins, *Polyhedron* **2001**, *20*, 2171–2177.
- [12] H. H. Sisler, N. L. Smith, *J. Org. Chem.* **1961**, *26*, 611–613.
- [13] O. Köhl, T. Koch, F. B. Somoza Jr, P. C. Junk, E. Hey-Hawkins, D. Plat, M. S. Eisen, *J. Organomet. Chem.* **2000**, *604*, 116–125.
- [14] a) M. T. Gamer, P. W. Roesky, *Inorg. Chem.* **2004**, *43*, 4903–4906; b) P. W. Roesky, *Inorg. Chem.* **2006**, *45*, 798–802; c) N. Poetschke, M. Nieger, M. A. Khan, E. Niecke, M. T. Ashby, *Inorg. Chem.* **1997**, *36*, 4087–4093; d) P. W. Roesky, *Heteroat. Chem.* **2002**, *13*, 514–520; e) M. T. Gamer, P. W. Roesky, *Inorg. Chem.* **2005**, *44*, 5963–5965; f) C. Qi, S. Zhang, J. Sun, *J. Organomet. Chem.* **2005**, *690*, 2941–2946; g) T. K. Panda, M. T. Gamer, P. W. Roesky, *Inorg. Chem.* **2006**, *45*, 910–916; h) P. W. Roesky, M. T. Gamer, N. Marinos, *Chem. Eur. J.* **2004**, *10*, 3537–3542; i) P. W. Roesky, M. T. Gamer, M. Puchner, A. Greiner, *Chem. Eur. J.* **2002**, *8*, 5265–5271; j) D. Fenske, B. Maczek, K. Maczek, *Z. Anorg. Allg. Chem.* **1997**, *623*, 1113–1120.
- [15] a) C. Airoldi, D. C. Bradley, H. Chudzynska, M. B. Hursthouse, K. M. A. Malik, P. R. Raithby, *J. Chem. Soc., Dalton Trans.* **1980**, 2010–2015; b) X. Yu, S. Bi, I. A. Guzei, Z. Liu, Z.-L. Xue, *Inorg. Chem.* **2004**, *43*, 7111–7119; c) P. Renner, C. Galka, H. Memmler, U. Kauper, L. H. Gade, *J. Organomet. Chem.* **1999**, *591*, 71–77; d) see also ref.^[15a]
- [16] a) M. D. Fryzuk, H. D. Williams, S. J. Rettig, *Inorg. Chem.* **1983**, *22*, 863–868; b) F. A. Cotton, P. A. Kibala, *Acta Crystallogr., Sect. C: Cryst. Struct. Commun.* **1991**, *47*, 270–272.
- [17] One of the reviewers suggested that the dynamic behavior observed here could also be interpreted as the twisting of the phosphinoamide ligand without dissociation of the phosphorus moiety from the Zr center. Although this possibility could not be ruled out, we consider the coordination/dissociation process of the phosphinoamide ligands to be reasonable for the following reasons. First, a similar process was also proposed in the solution dynamics of Zr(Ph₂PNPh)₄ and (Ph₂PNR)₂TiCl₂. Second, the facile reaction with CuCl and other complex fragments suggests the existence of uncoordinated phosphorus atoms in solution.
- [18] C. Qi, S. Zhang, J. Sun, *Appl. Organomet. Chem.* **2006**, *20*, 138–141.
- [19] J. T. Gill, J. J. Mayerle, P. S. Wekker, D. F. Lewis, D. A. Ucko, D. J. Barton, *Inorg. Chem.* **1976**, *15*, 1155–1168.
- [20] One reviewer suggested that the CO stretching vibration in the IR spectrum could also be shifted as a result of the geometric constraints given by the tripodal phosphorus ligand. This cannot be ruled out.
- [21] a) F. A. Cotton, G. Wilkinson, P. L. Gaus (Eds.), *Basic Inorganic Chemistry*, 3rd ed., John Wiley & Sons, New York, **1995**, pp. 60–61; b) A. Bondi, *J. Phys. Chem.* **1964**, *68*, 411–451; c) R. D. Shannon, *Acta Crystallogr., Sect. A* **1976**, *32*, 751–767.
- [22] D. P. Tate, W. R. Knipple, J. M. Augl, *Inorg. Chem.* **1962**, *1*, 433–434.
- [23] H. C. Clark, L. E. Manzer, *J. Organomet. Chem.* **1973**, *59*, 411–428.
- [24] The extreme moisture sensitivity of the complex prevented its exact elemental analysis even though we used our best techniques, including sample preparation in a glove box, weight measurement in a glove bag, and elemental analysis as soon as the weight measurement was complete.
- [25] A. Altomare, M. Burla, M. Camalli, G. Cascarano, C. Giacovazzo, A. Guagliardi, A. Moliterni, G. Polidori, R. Spagna, *SIR97*, **1999**.
- [26] A. Altomare, G. Cascarano, C. Giacovazzo, A. Guagliardi, M. Burla, G. Polidori, M. Camalli, *SIR92*, **1994**.

- [27] P. T. Beurskens, G. Admiraal, G. Beurskens, P. W. Bosman, R. de Gelder, R. Israel, J. M. M. Smits, *The DIRDIF-99 Program System: Technical Report of the Crystallography Laboratory*, University of Nijmegen, Nijmegen, The Netherlands, **1999**.
- [28] D. T. Cromer, J. T. Waber, *International Tables for X-ray Crystallography*, Kynoch Press, Birmingham, U. K., **1974**, vol. 4.
- [29] *Crystal Structure 3.8: Crystal Structure Analysis Package*, Rigaku and Rigaku/MSK, 9009 New Trails Dr., The Woodlands, Texas, 77381 USA, **2000–2006**.
- [30] J. R. Carruthers, J. S. Rollett, P. W. Betteridge, D. Kinna, L. Pearce, A. Larsen, E. Gabe, *CRYSTALS Issue 11*, Chemical Crystallography Laboratory, Oxford, U. K., **1999**.

Received: January 3, 2007

Published Online: May 15, 2007